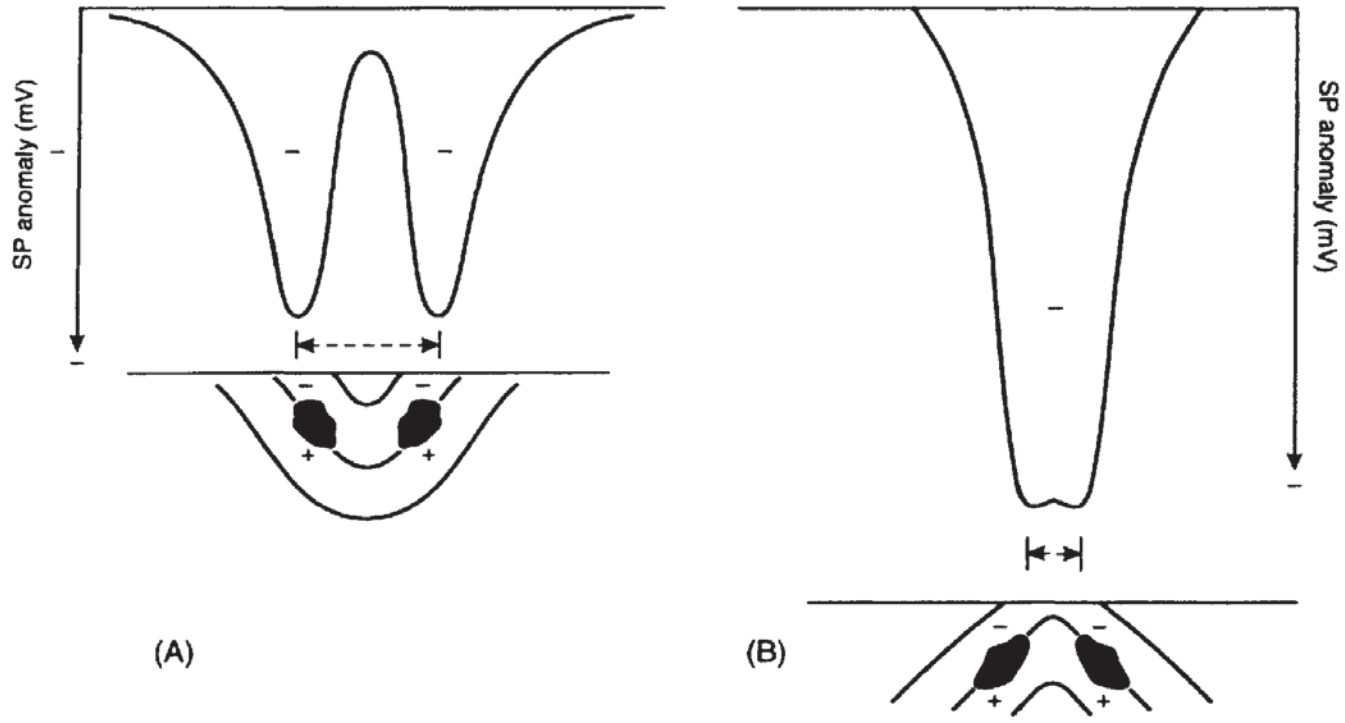

Figure 8.7 SP anomalies due to (A) two graphite bodies with axes of polarisation inclined away from each other (in syncline), and (B) inclined towards each other (in anticline). After Meiser (1962), by permission

and their respective SP anomalies are shown in Figure 8.9. The observed anomaly in Figure 8.9B is the envelope of the anomalies due to the individual geological components A–D.

8.7 APPLICATIONS AND CASE HISTORIES

8.7.1 Geothermal

The hydrogeological regimes associated with geothermal fields are often complex. Water bodies can have highly differing temperatures and salinities, and be highly mobile (e.g. Cioni *et al.* 1992). Consequently, streaming potentials may be well developed and hence may be measured using the SP method (see also Anderson and Johnson (1976) and Zohdy *et al.* (1973)).

8.7.1.1 Roosevelt Hot Springs, Utah, USA

A self-potential profile carried out across the Dome Fault Zone, Roosevelt Hot Springs, Utah, is shown in Figure 8.10 (Corwin and Hoover 1979). Alunite and pyrite occur in the zone, both of which normally produce negative polarity anomalies that may be evident on the profile within 1 km west of the reference electrode position. The area within 1 km to the east of the reference electrode has a positive anomaly of about +80 mV which is thought to be due to the

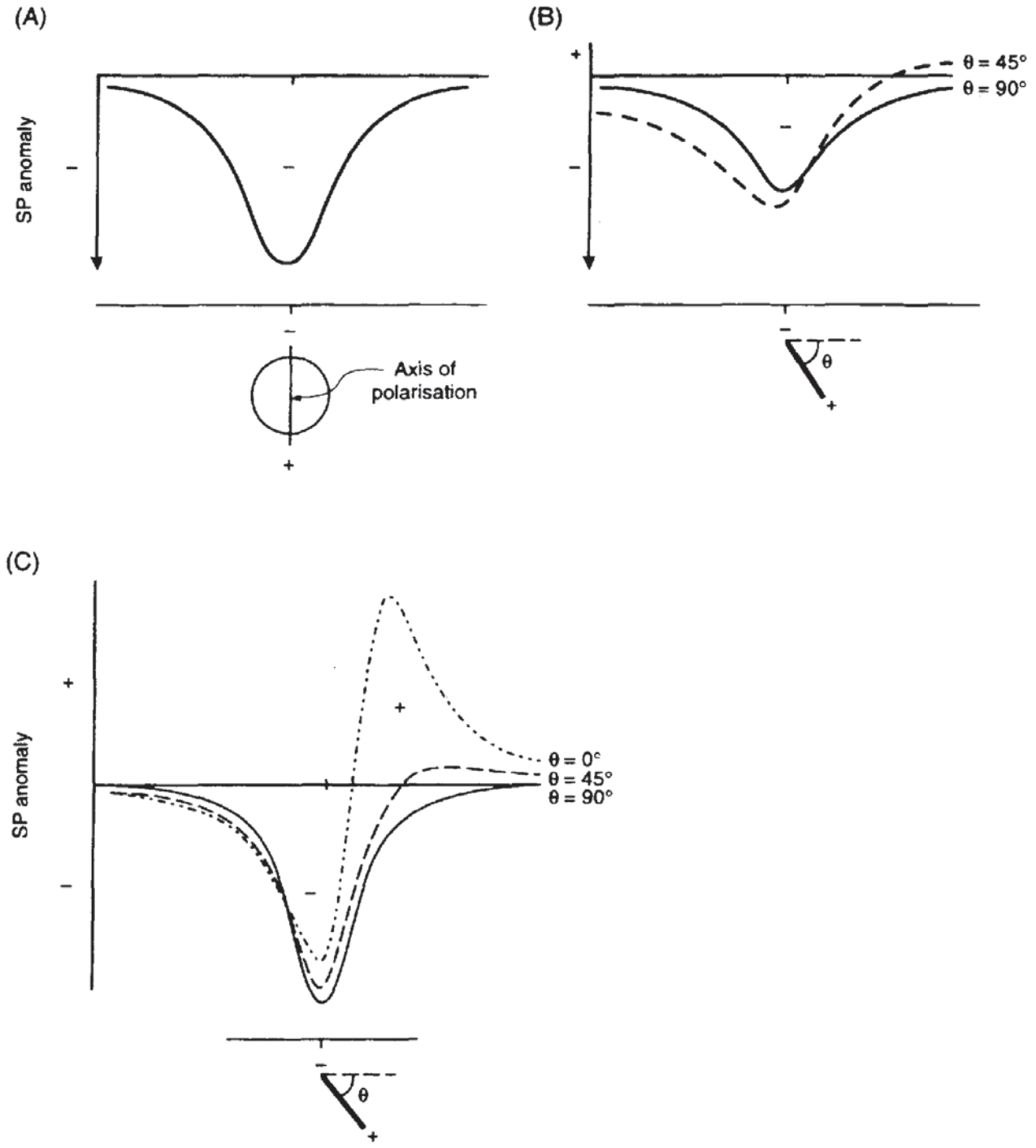

Figure 8.8 Self-potential anomalies associated with (A) a sphere, (B) a dipping plate (Parasnis 1986), and (C) a dipping rod (Telford *et al.* 1990)

geothermal activity. Comparison of the thermal gradient profile with the SP transect indicates that the axis of the thermal gradient anomaly is coincident with the position of the reference electrode. The negative potentials associated with the mineralised areas within the zone may be degrading the anomaly due to the geothermal activity. The geothermal SP anomaly results from streaming

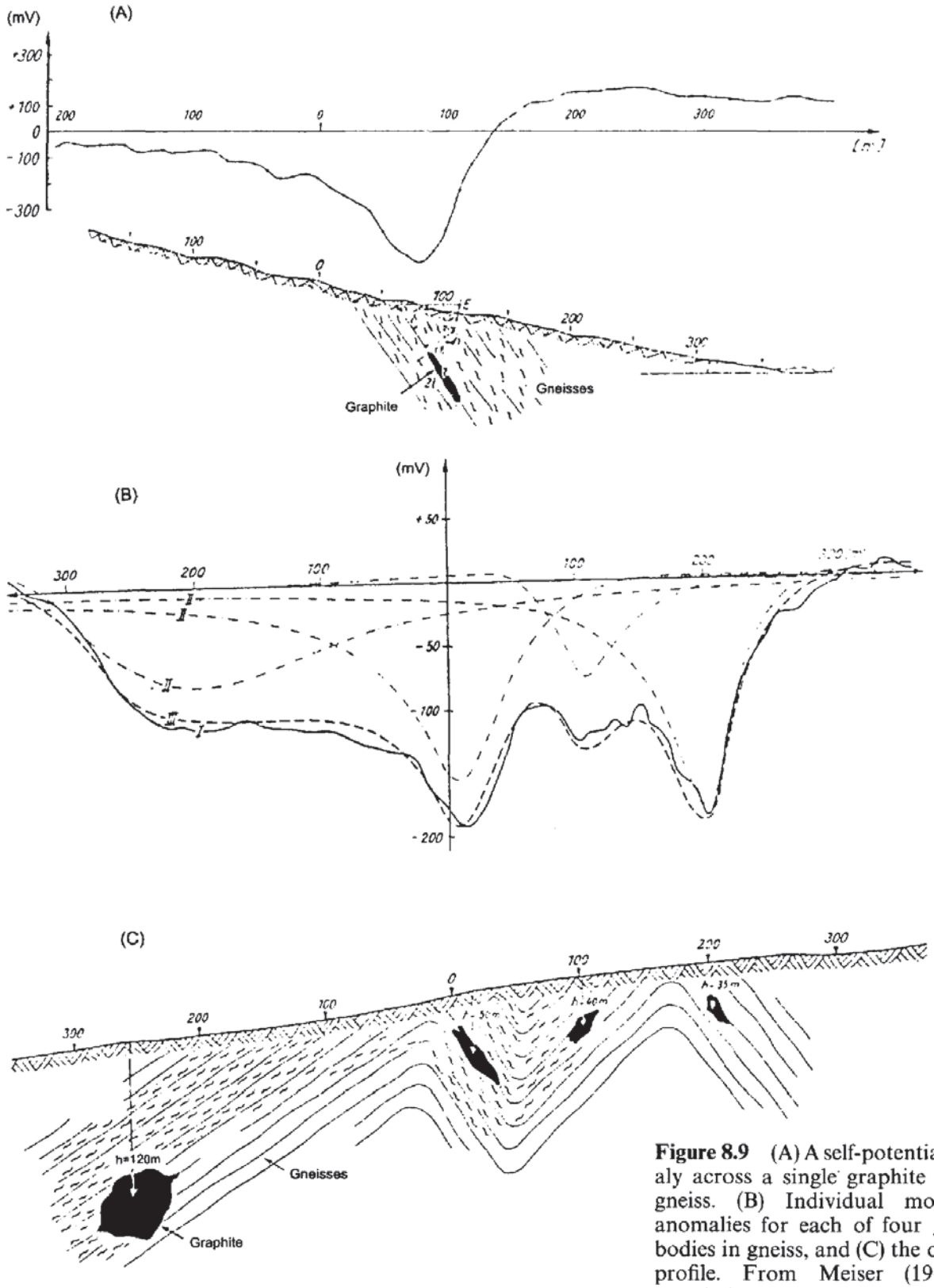

Figure 8.9 (A) A self-potential anomaly across a single graphite body in gneiss. (B) Individual model SP anomalies for each of four graphite bodies in gneiss, and (C) the observed profile. From Meiser (1962), by permission

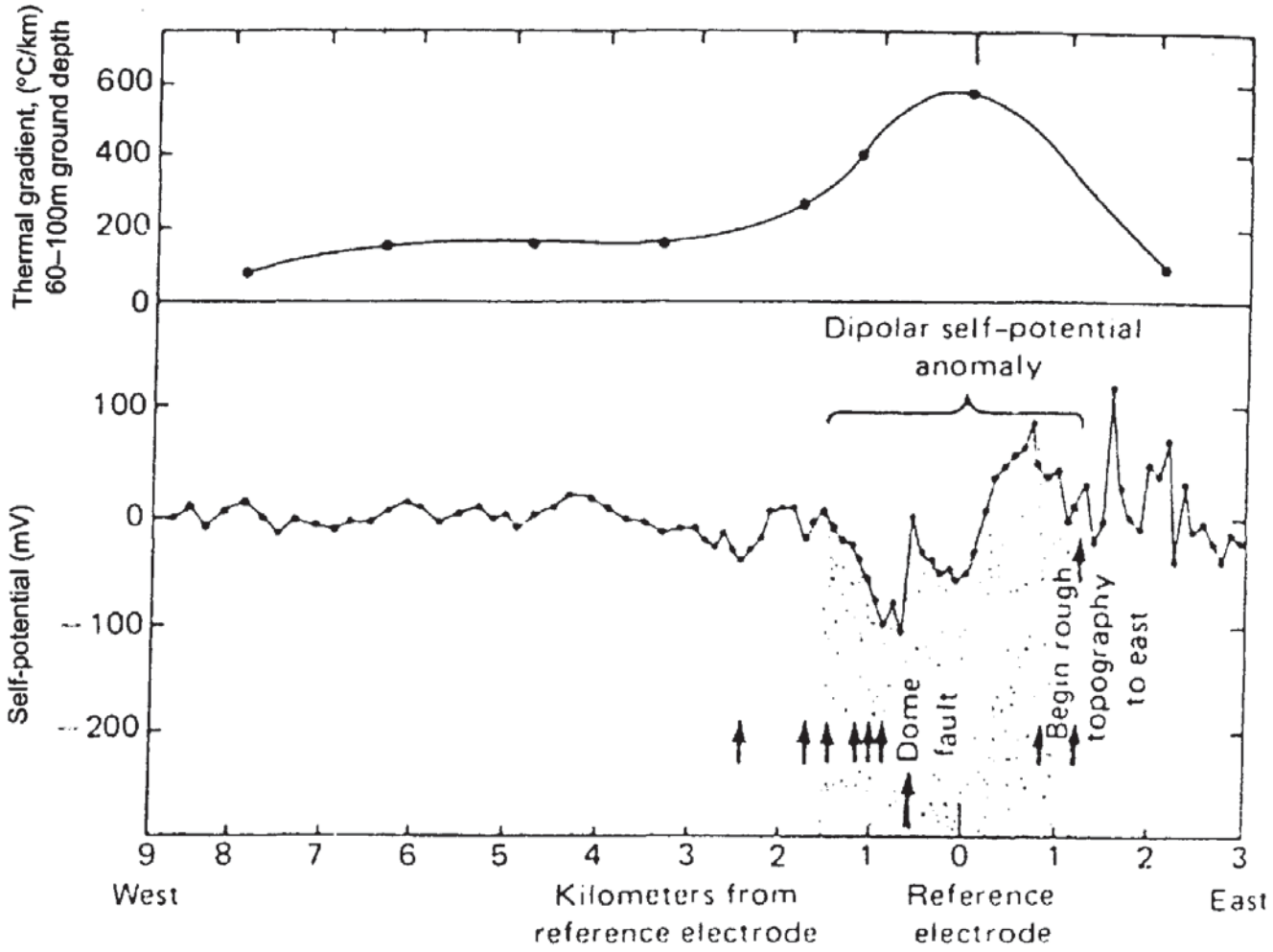

Figure 8.10 Thermal gradient and self-potential profiles over the Dome Fault Zone, Roosevelt Hot Springs, Utah. Arrows denote points at which mapped faults cross the SP survey line. From Corwin and Hoover (1979), by permission

potentials being driven by the convective cells within such a zone and also from elevated diffusion potentials due to the higher temperatures.

8.7.1.2 Cerro Prieto geothermal field, Mexico

Corwin and Hoover (1979) have reported on a significant SP anomaly of some 150 mV peak-to-peak amplitude associated with the Cerro Prieto geothermal field in Mexico (Figure 8.11). The anomaly is centred over the Hidalgo Fault which is thought to provide a major conduit for geothermal fluids. The actual geology of the field is still not fully understood, but it is clear that the production zone, which generates about 75 MW of electrical energy, is located between the maximum and minimum points of the SP anomaly which are 8 km apart (Fitterman and Corwin 1982). The width of the SP anomaly is possibly owing to several faults acting as geothermal conduits rather than just the Hidalgo Fault.

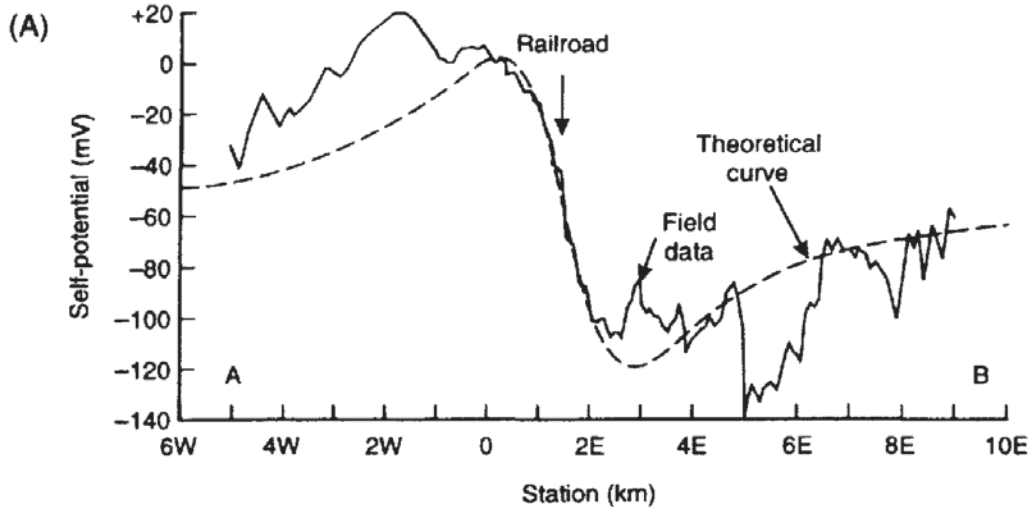
(A)
Railroad
Theoretical curve
Field data
Self-potential (mV)
+20
0
−20
−40
−60
−80
−100
−120
−140
A
B
6W
4W
2W
0
2E
4E
6E
8E
10E
Station (km)

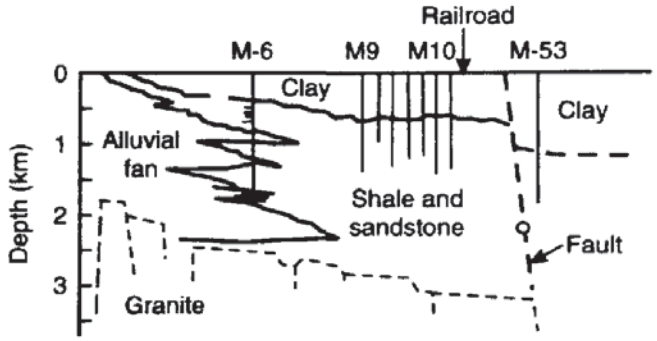
Railroad
M-6
M9
M10
M-53
Clay
Clay
Alluvial fan
Shale and sandstone
Fault
Granite
Depth (km)
0
1
2
3

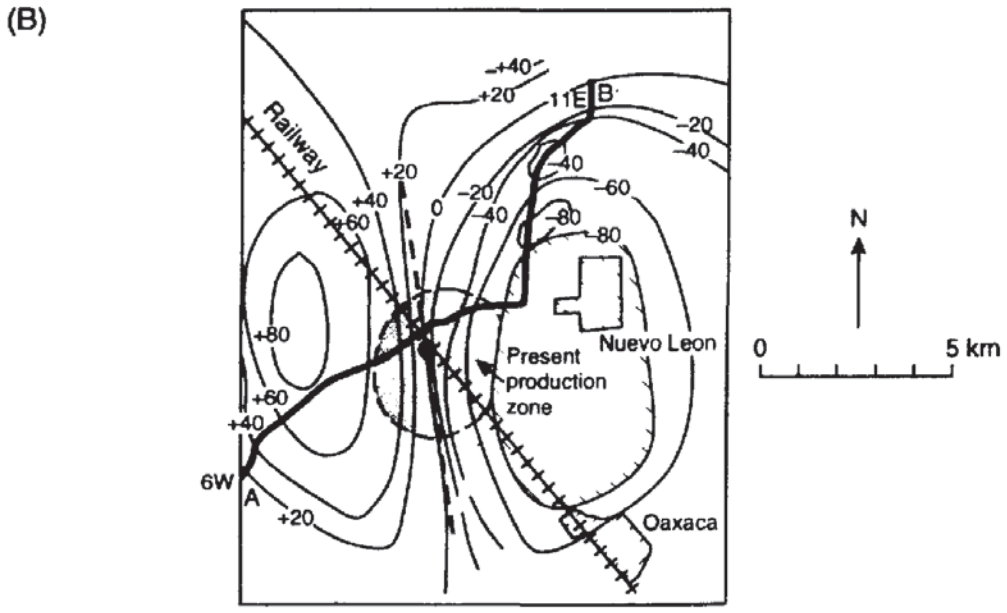
(B)
Railway
+40
+20
11E
B
−20
−40
+20
+40
+60
0
−20
−40
−40
−60
−80
−80
+80
+60
+40
6W
A
+20
Present production zone
Nuevo Leon
Oaxaca
N
0
5 km

8.7.2 Location of massive sulphide ore bodies

8.7.2.1 Kimheden orebody, Skellefte, northern Sweden

The Kimheden orebody, which is mainly pyrite, occurs in steeply dipping sheets along a ridge in moraine-covered sericite–quartzite. The tops of the ore fragments are at no more than about 10 m depth. The SP contours (Figure 8.12) show several clear linear features which correlate extremely well with the known position of the

Figure 8.11 (*opposite*) (A) Self-potential anomaly along the profile A–B over the Cerro Prieto Geothermal Field, Mexico, with a simplified geological cross-section. After Corwin and Hoover (1979), by permission. (B) Self-potential map over the same field (profile line A–B marked) showing a distinct positive–negative couplet with the geothermal production area being midway between the two parts of the anomaly. After Fitterman and Corwin (1982), by permission

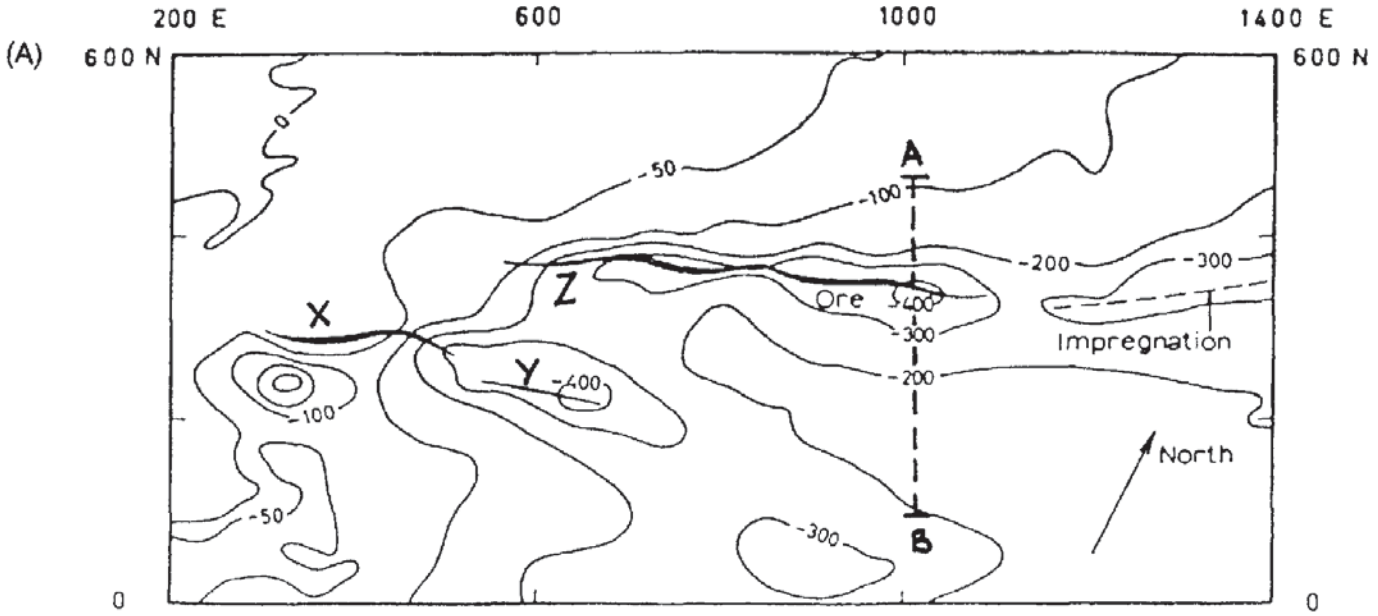

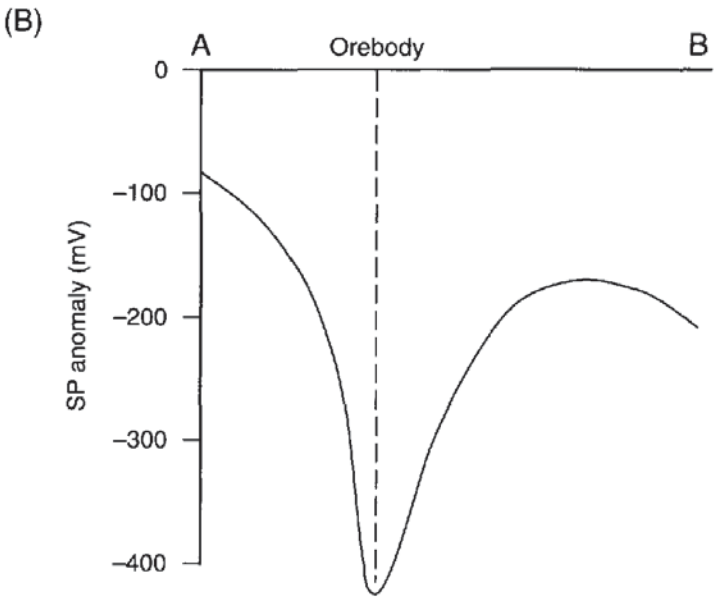

Figure 8.12 (A) Self-potential map of the Kimheden pyrite orebody in northern Sweden. From Parasnis (1966), by permission. (B) The SP anomaly across profile A–B. Map contours are in mV

orebodies (Parasnis 1966) with one exception. The most western orebody (X) was found to have a particularly high resistivity which may explain the absence of any anomaly (see Section 8.3.3).

Figure 8.13 (*opposite*) (A) Map of the solid geology and self-potential values (in mV) in Chalkidiki, northern Greece. (B) SP and magnetic total field anomaly (in nT) profiles r–r' and Δ–Δ. From Zachos (1963), by permission

8.7.2.2 Copper ore at Chalkidiki, northern Greece

The Chalkidiki area of northern Greece consists of gneisses and schists that are strongly sheared and intruded by mineralised granitic–granodioritic and ultrabasic structures (Figure 8.13). Pyrite, galena and sphalerite are associated with the acidic intrusions, and magnetite and chromite with the basic intrusions. Copper minerals and pyrite have resulted from Tertiary volcanic activity and are particularly associated with lava flows of trachytes, andesites and porphyritic granodiorite, and have been concentrated within a dense network of fractures and faults. There are three recognisable zones of copper mineralisation of which the shallowest consists of an oxidised leached zone (about 1% Cu). Below this is a zone of secondary enrichment 2–3 m thick in which copper concentrations are as high as 20% (malachite, azurite, cuprite, etc.). The lowest zone, which represents the primary mineralisation of chalcopyrite, pyrite, bornite and *syngenetic magnetite, begins at around 20–30 m depth and extends down to at least 300 m below surface. The magnetite within the volcanic rocks gives rise to distinctive magnetic anomalies, the maxima of which occur just within the margins of the trachyte dome. The minima of the self-potential anomalies occur specifically over the copper orebodies. Where the oxidisation of the copper sulphide is marked, which produces a low magnetic susceptibility, there is a corresponding cusp in the magnetic profile. This example also highlights the complementary use of two different geophysical methods (based on Zachos (1963) and Parasnis (1966)).

8.7.2.3 Sulphide orebody at Sariyer, Turkey

A classic, and oft cited, example of a self-potential anomaly over a sulphide orebody is the one given by Yüngül (1954) for a complex orebody at Sariyer in Turkey (Figure 8.14A). Chalcopyrite and pyrite occur in varying concentrations within a massive deposit within andesite and below Devonian schist. The area is characterised by a steep surface gradient which, if not corrected for, displaces the SP minimum downhill. The orebody comprises four regions, of which the one furthest downhill is pyritised and the three remaining zones have decreasing concentrations of copper from 14% on the downhill side to 1–2% on the upslope side. Each of these zones may be represented by a sphere whose SP anomaly contributes to the total anomaly observed (Figure 8.14B). The inflection points present on the observed profile can be modelled by changing the separation between the various model spheres.

(A)

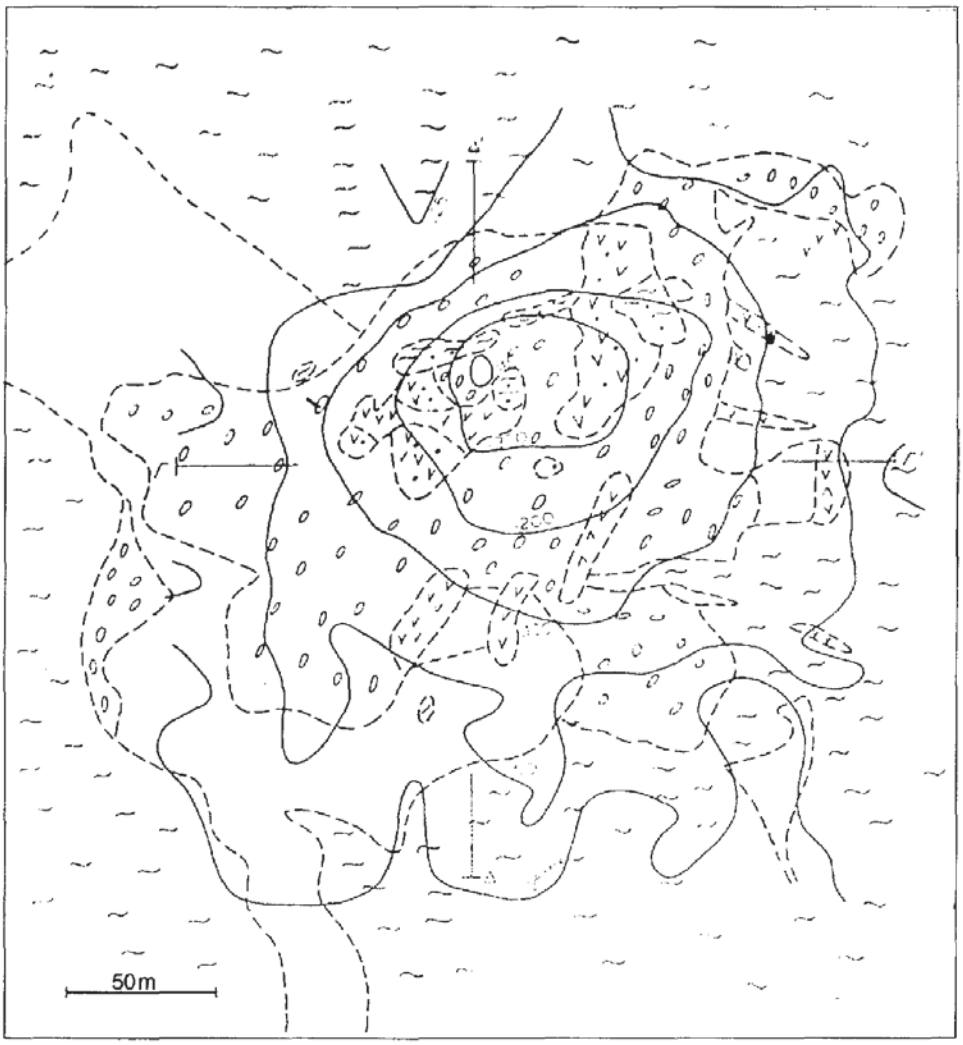
50m

(B)

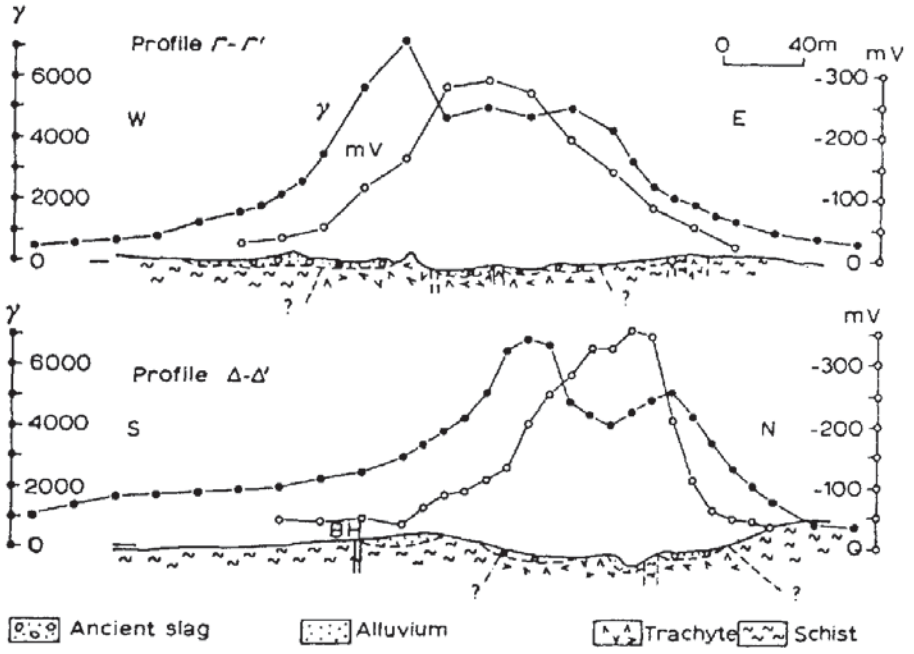
γ
Profile Γ-Γ'
0 40m
mV
6000
4000
2000
0
W
E
-300
-200
-100
Profile Δ-Δ'
S
N
BH
Ancient slag
Alluvium
Trachyte
Schist

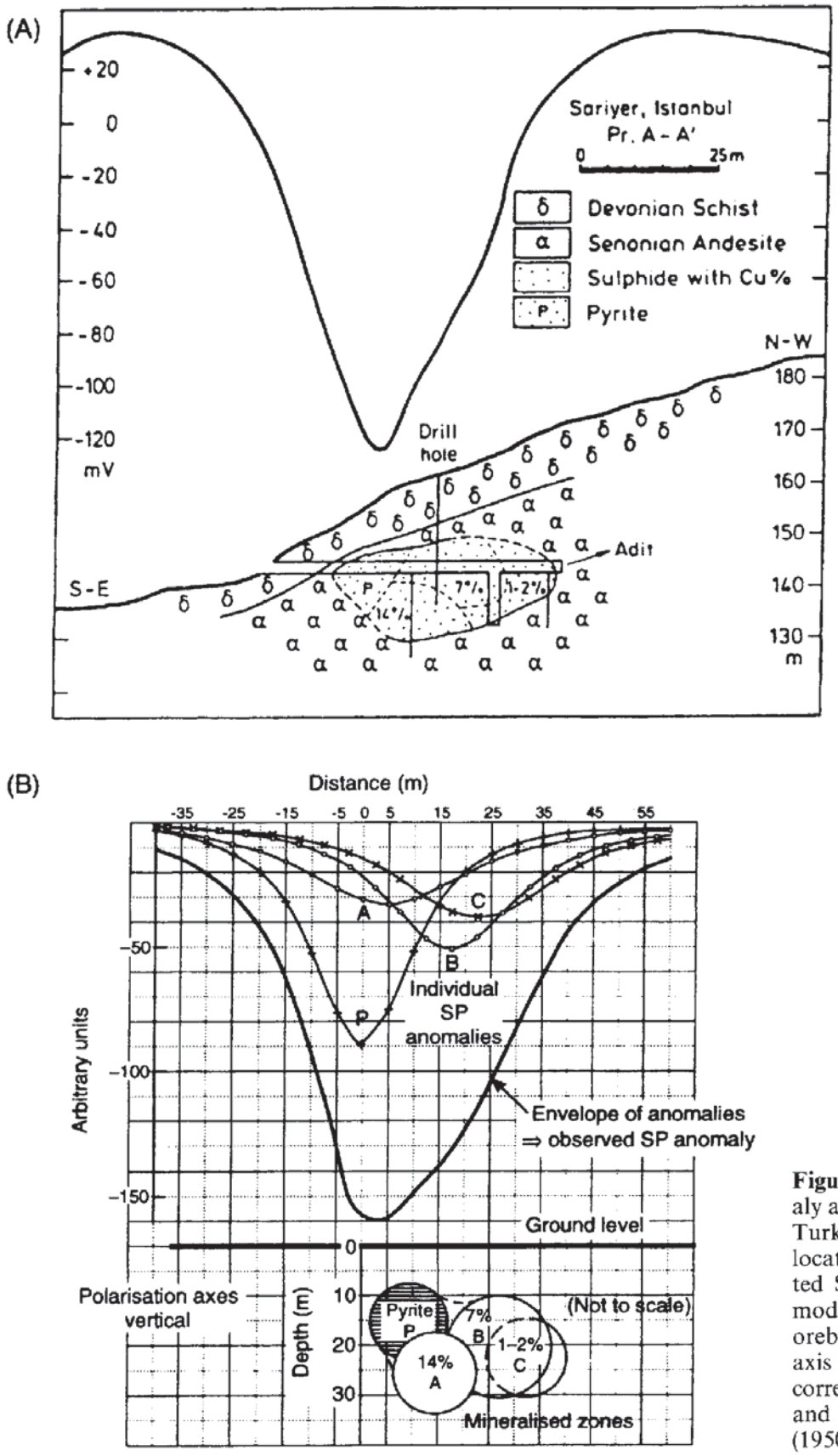

Figure 8.14 (A) Self-potential anomaly across a pyrite orebody at Sariyer, Turkey. The borehole is located at the location of the topographically corrected SP minimum. (B) An equivalent model assuming each segment of the orebosy conforms to a sphere with its axis of polarisation vertical with the corresponding individual SP anomalies and their envelope. After Yüngül, (1950), by permission

This example demonstrates that subtle inflection points within an anomaly may be extremely important and should not be dismissed as being insignificant. In addition, the field data must be of very high quality in order to isolate such subdued features. For another example of the use of SP data in pyrite orebody investigations, see Logn and Bölviken (1974).

8.7.3 Hydrogeology

Geothermal applications involving groundwater have already been discussed (Section 8.7.1) and the use of SP measurements in groundwater borehole testing were mentioned in Section 8.3.1. Other examples in hydrogeology are the use of SP measurements to detect the sites of leakages associated with man-made and natural dams (Ogilvy *et al.* 1969; Bogoslovsky and Ogilvy 1970a,b; Butler and Llopis 1990; Jansen *et al.* 1994), percolation of fresh groundwater through quartz gravels (Nayak 1981), and in the study of groundwater movement (Schiavone and Quarto 1984), for example.

A recent example of a more regional SP survey has been given by Fournier (1989) who has used the method in conjunction with electrical resistivity surveys to investigate the hydrogeology of volcanic aquifers in the Chaîne des Puys area of central France. He was able to delimit the catchment area of each spring, and found that an axial graben was the main aquifer and identified possible zones vulnerable to pollution. He also found that the water table provided the main source of SP anomalies and that their shape indicated the form of the water table (Figure 8.15). A geological cross-section of part of northern Chaîne des Puys, with its corresponding SP profile, is shown in Figure 8.16. Note that the negative maximum coincides with the topographic high. For the area, Fournier was able to categorise his SP anomalies in terms of hydrogeological significance (Table 8.3). It remains to be seen how applicable these associations are for other geographic areas.

Associated with the hydrogeological applications of SP measurements, is their possible use in earthquake prediction where the active fault planes are at very shallow depths and where instrumentation is both feasible and viable. It has been noted previously (Rikitake 1976) that natural electric fields within the ground may change prior to an earthquake, and therefore could act as sensible precursors to some types of seismic events. Renata (1977) has attempted to argue that these electrical changes may be due to electrokinetic potentials associated with stress buildup/relaxation processes.

Further evidence of what is now called the 'seismoelectric response' has been presented by Butler *et al.* (1994). In an experiment using a sledge hammer source and electric field receivers, an electromagnetic signal was observed when the seismic wave impinged upon a boundary between organic-rich fill and impermeable glacial till. The

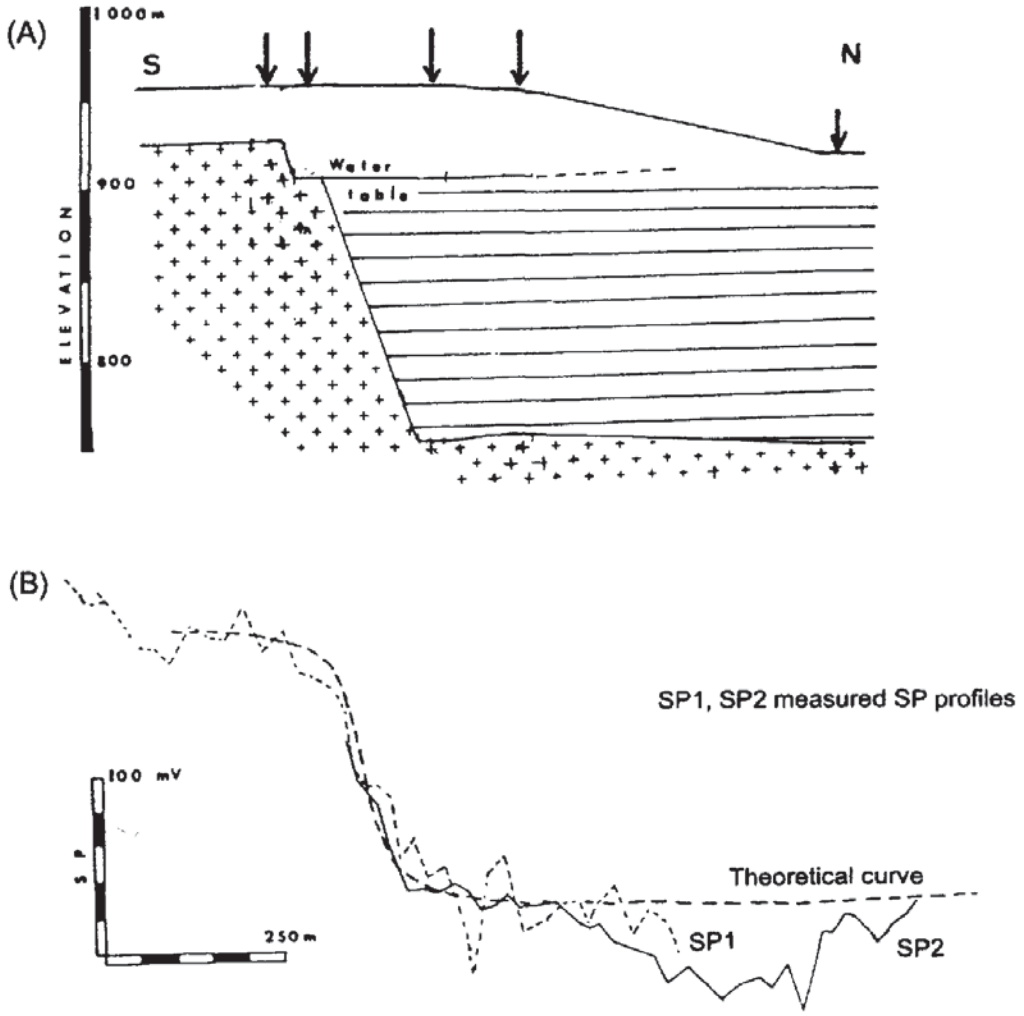

Figure 8.15 (A) Geological cross-section of part of the axial graben in the Chaîne des Puys, central France, as derived from vertical electrical soundings (arrows). (B) The corresponding self-potential anomaly. From Fournier (1989), by permission

depth to the interface (confirmed by drilling) was from 1 m to 3 m. It is believed that the electrical response was a transient streaming potential produced by a seismically induced flow of pore water at the interface. The critical combination in this experiment was the juxtaposition of a permeable material and an aquitard at shallow depth. It is postulated that this technique could be used to help map aquitards or the boundaries of permeable formations where they terminate against an impermeable material.

8.7.4 Landfills

Steep-sided landfills containing significant volumes of highly conductive leachate which may leak through the margins are known to generate significant SP anomalies (Coleman 1991). The reasons for this are primarily twofold. First, there is an ionic imbalance in concentrations each side of the landfill boundary, with high values within the landfill (due to the leachate) and low values outside (within

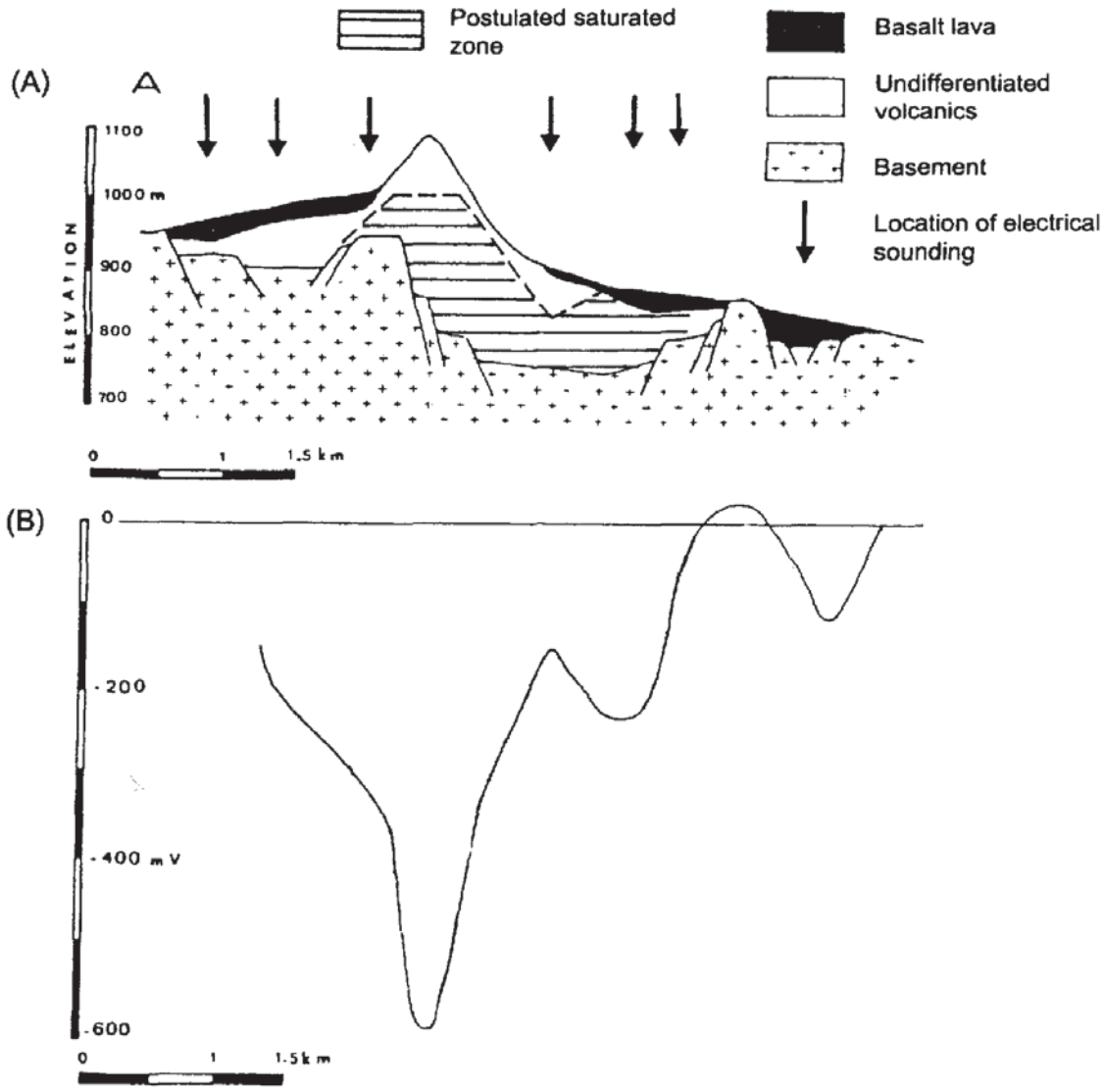

Figure 8.16 (A) Geological cross-section across a volcanic dome in the northern part of the Chaîne des Puys, central France, as derived from vertical electrical soundings (arrowed. (B) The corresponding self-potential anomaly. From Fournier (1989), by permission

Table 8.3 Hydrogeological interpretation of SP anomalies (Fournier 1989)

Aspect	Location	Hydrogeological significance
High horizontal SP gradient	On flat topography	Lateral limit of an unconfined acquifer
	On a volcano flank	Ascent of water table in volcanic cone
SP minimum	On flat topography	Palaeovalley axis
	On a volcano flank or summit	Crest of the water table and underground watershed line
SP maximum	Above an unconfined acquifer	Depression of the water table due to better drainage
	Between two unconfined acquifers	Watershed line due to crest of the impervious basement

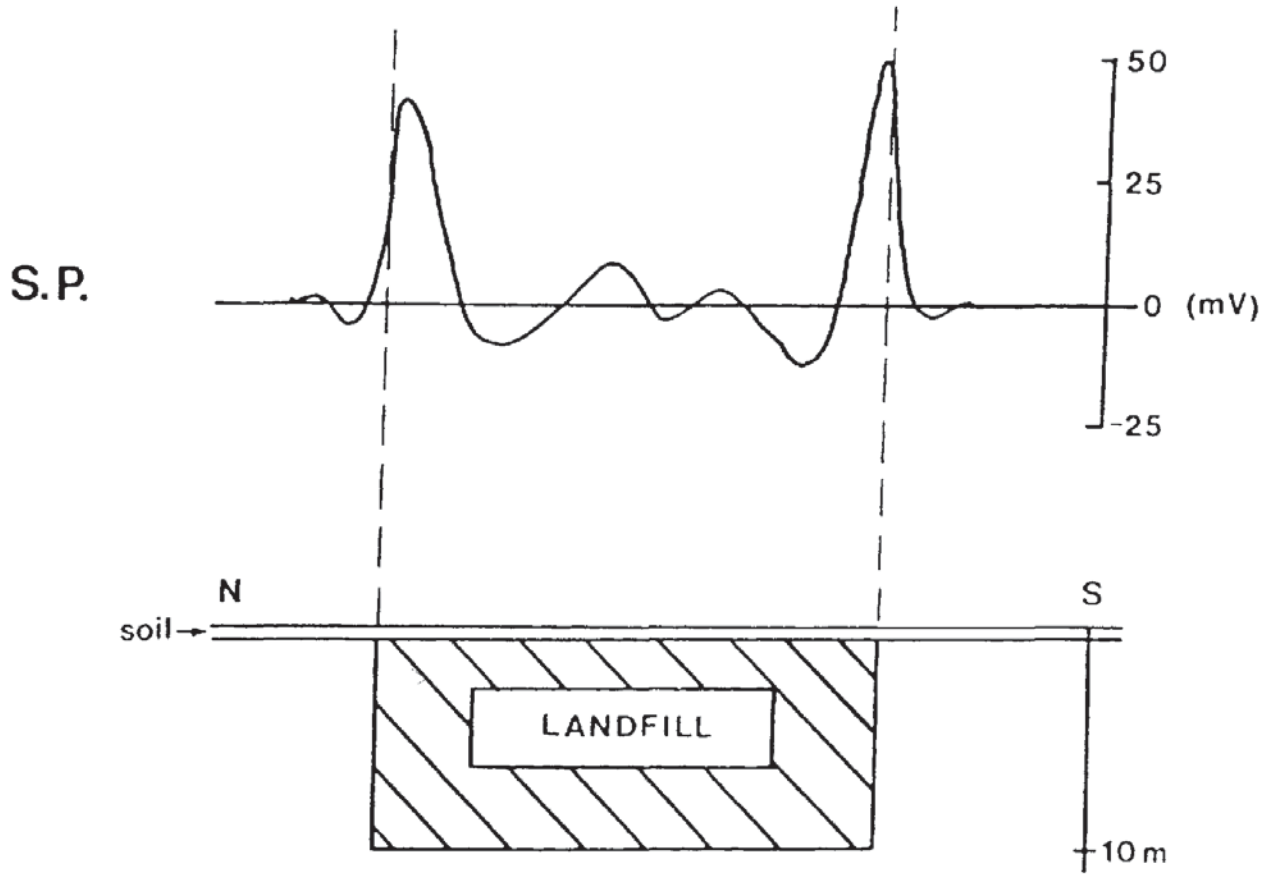

Figure 8.17 SP anomaly over a closed landfill, showing the typically larger anomalies associated with the landfill boundaries compared with those observed in the interior. From Coleman (1991), by permission

the natural groundwater). In order to equilibrate the imbalance, diffusion occurs. As ions (which are charge carriers) move, their movement constitutes an electromotive force – an electrochemical potential. Secondly, if the leachate physically flows from the landfill outwards, a streaming potential may be generated. Consequently, if both electrochemical and streaming potentials are generated, it is highly probable that a measurable SP anomaly would be present at the landfill boundaries.

Coleman (1991) has produced an example of SP anomalies associated with the margins of a landfill (Figure 8.17). While there are small SP anomalies within the landfill, the largest SP events are associated with the boundaries, where the ionic imbalances are greatest and the rate of flow of leachate is most pronounced.

8.7.5 Leak detection within embankments

The SP method has been used to detect leaks in earth dam embankments for decades (e.g. Bogoslovsky and Ogilvy, 1970a,b). Although less well publicised, marine or boat-borne SP surveys have been made for at least 60 years. Where groundwater flows through such a structure by finding the path of least resistance (e.g. piping), electrokinetic

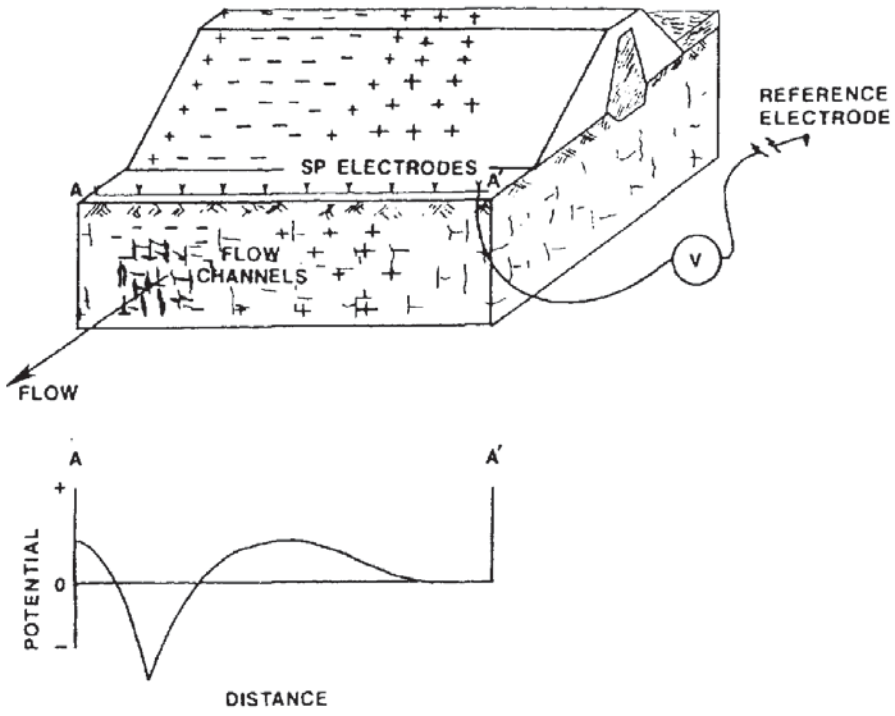

Figure 8.18 Schematic of the concept of SP anomalies generated by features associated with seepages through earth dams. From Butler and Llopis (1990), by permission

streaming potentials may be generated with sufficient magnitude to be detectable. The concept of the generation of SP anomalies by leaks is shown schematically in Figure 8.18. Negative charges are associated with locations where leaks enter a dam, or above seepage paths where the flow is generally horizontal or descending. In contrast, positive anomalies may occur where the flow is generally ascending and where surface seepage takes place. Consequently, the presence of either or both a negative and/or positive anomaly may be physically significant.

Butler and Llopis (1990) have described an example of an SP survey to examine possible leaks at the Mill Creek Dam and Reservoir, Washington, USA (Figure 8.19). Since its first test filling in 1941, considerable loss of stored water has been noticed. Attempts to change or stop the seepage have been unsuccessful. A concrete cutoff wall with flanking grout curtains was installed. The concrete wall was built on top of a massive basalt which underlies laterally variable conglomerate. Since the construction of these structures, the reservoir had not been filled but seepage was still evident.

In 1984, a geophysical investigation was instigated to detect anomalous seepage before, during and after test filling of the reservoir. Two SP electrode arrays comprising 85 metallic rods (copper-clad steel grounding rods) at 15 m spacings were installed two months before the first set of SP readings and four months before the first test filling. The reference electrode was located upstream. During the test, the reservoir level was raised by 10 m. The SP profile acquired along

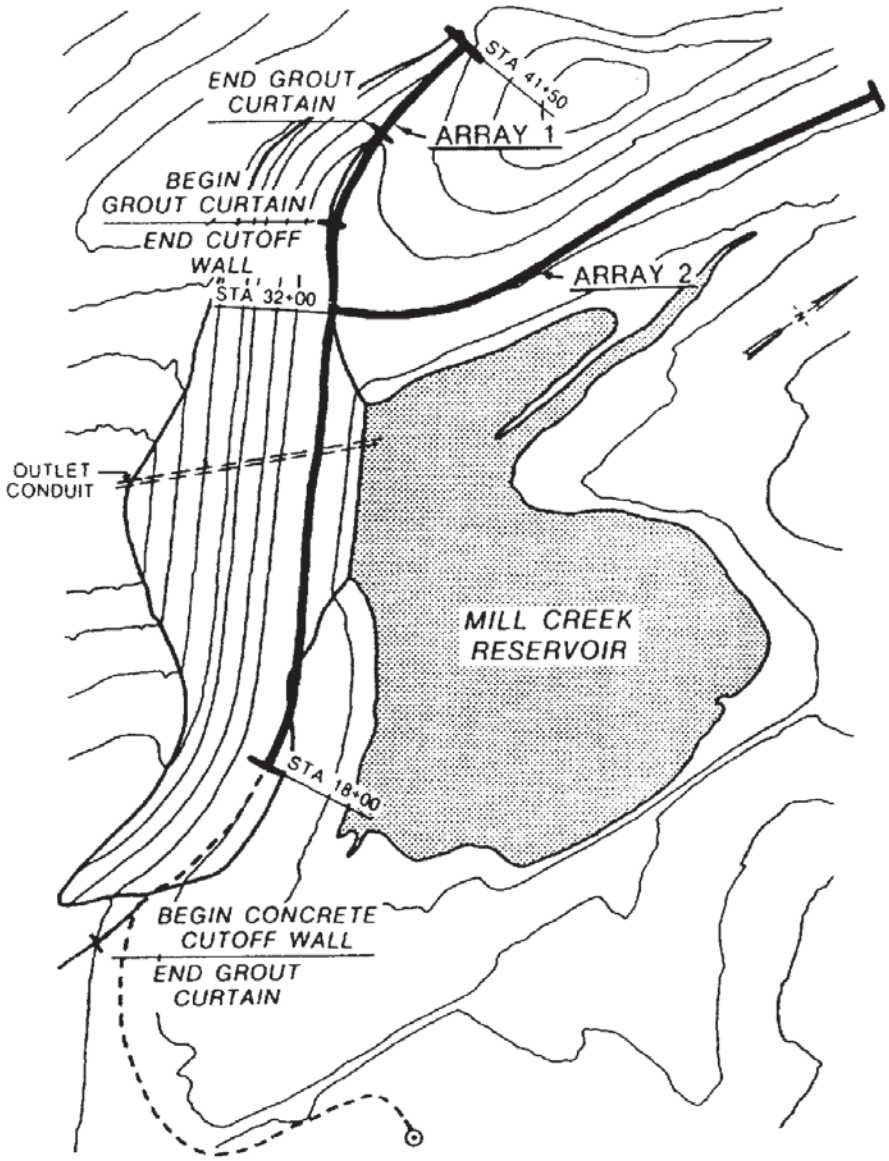

Figure 8.19 Plan of Mill Creek Dam and Reservoir, Washington, USA, showing the locations of SP survey lines 'Array 1' and 'Array 2', grout curtains and the concrete cutoff wall. From Butler and Llopis (1990), by permission

Array 1 (see Figure 8.19) before the filling of the reservoir is shown in Figure 8.20. Several notable features are evident:

- There is an anomaly of about −380 mV associated with a 1.07 m diameter outlet conduit located about 20 m below the electrode array.
- Three separate zones along Array 1 are distinguished by different base levels (indicated by dashed lines).
- The boundaries between zone 1/zone 2 and zone 2/zone 3 coincide approximately with the dam/right abutment contact and the end of the grout curtain, respectively. The anomaly associated with the boundary between zone 1 and zone 2 is thought to be due to a lateral change in material type. The zone 2/zone 3 boundary is

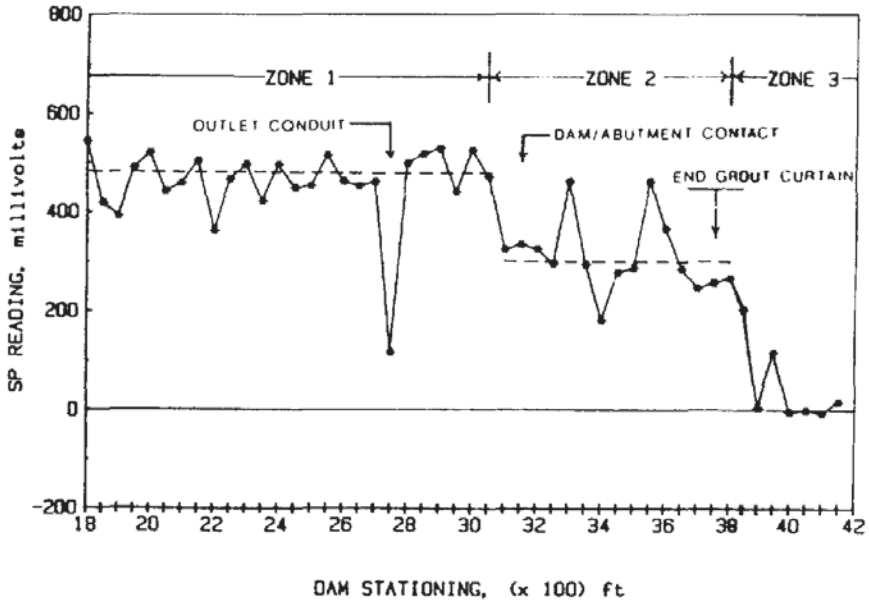

Figure 8.20 Array-1 SP data acquired prior to the start of the filling of the Mill Creek Reservoir in Figure 8.19. From Butler and Llopis (1990), by permission

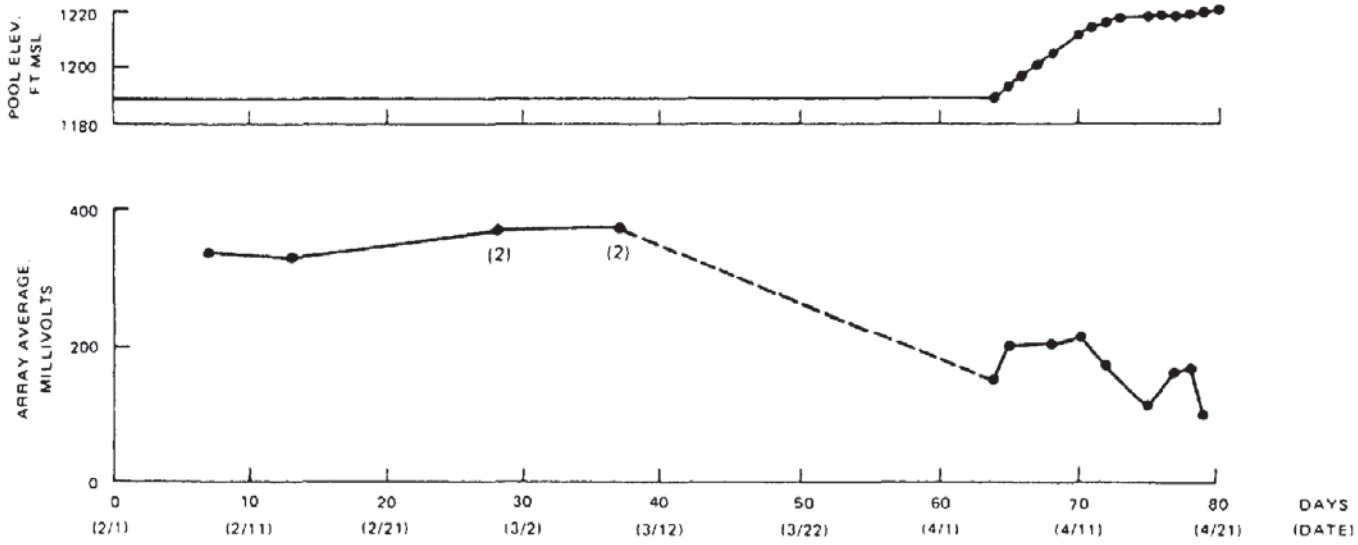

Figure 8.21 Comparision of the reservior water level with SP array average as a function of time (see Figure 8.19). Raising of the water level started on the 5th day of April (4/5). From Butler and Llopis (1990), by permission

caused by a lateral change in the groundwater flow regime as a result of the presence of the cutoff wall and the grout curtain.

As a test of the SP response to the raising of the level of the reservoir, values of the array averages responded immediately to the increase in water level, as indicated by the data in Figure 8.21. No SP values were measured between 9 February and 5 March; the test fill began on 5 March. Note that the trend in SP anomaly with time is negative.

Further analysis of the SP data yielded an indication of several locations, most notably at location 18 (Figure 8.20) and at 30 + 50.

(A)

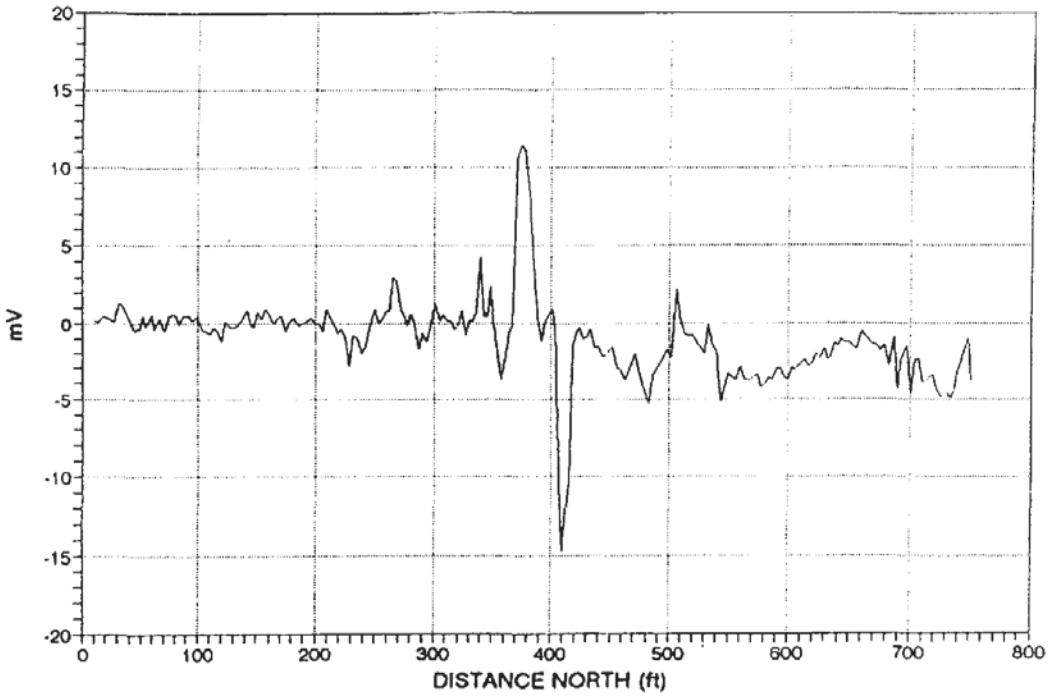
20
15
10
5
0
-5
-10
-15
-20
mV
0
100
200
300
400
500
600
700
800
DISTANCE NORTH (ft)

(B)

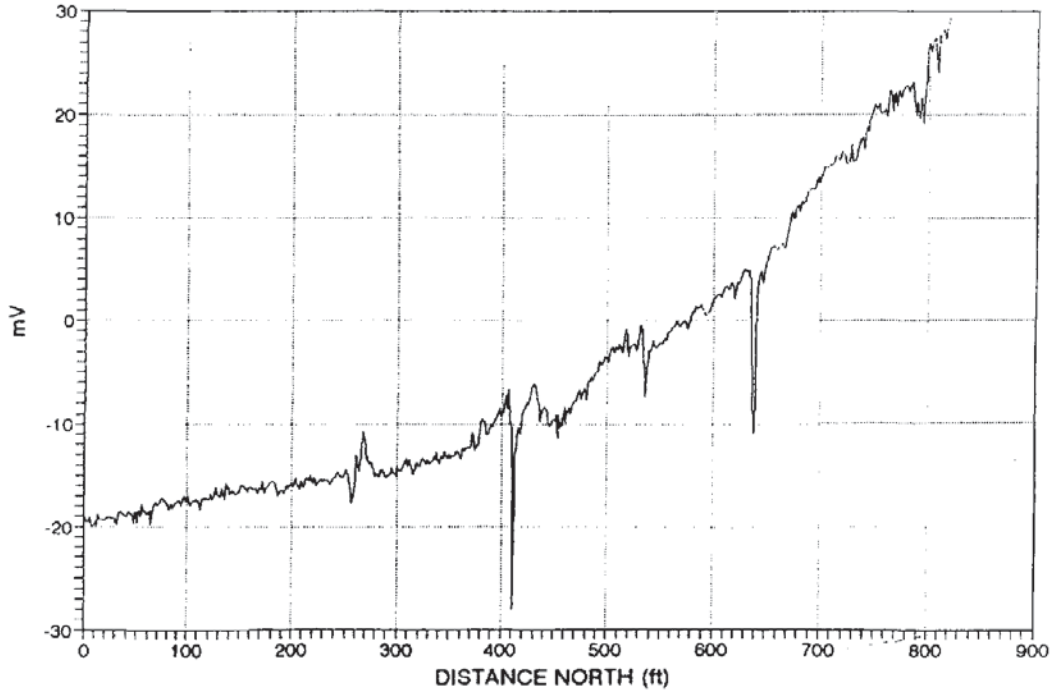
30
20
10
0
-10
-20
-30
mV
0
100
200
300
400
500
600
700
800
900
DISTANCE NORTH (ft)

The cause at station 18 was thought to be seepage occurring under the cutoff wall in a very localised zone. The postulated seepage at 30 + 50 coincides with the end of the cutoff wall/grout curtain. The SP data, although not conclusive in themselves, provided valuable spatial and temporal data which aided a better understanding of the hydrological conditions of the site.

Marine surveys have been undertaken typically with a pair of electrodes (gradient array) behind a boat towed at the surface or at depth above the water bottom. Alternatively, using an electrode fixed on the water bottom, a mobile electrode is dragged along the bottom. Occasionally, a borehole SP logging tool is used as the mobile tool. Other configurations include a pair of electrodes separated by only 1.25 m, suspended beneath a boat or lowered to the water bottom and are used with a third, fixed electrode planted by a diver remote from the profile line. An alternative to the surface-towed gradient arrays is the benthic gradient array where two electrodes are towed behind a weighted towfish and are dragged along the water bottom in direct contact with the sediment. A development of this is the use of a fixed electrode, implanted by deploying the weighted electrode from the boat and letting it sink under gravity, and towing a weighted eel with a second electrode in its hind part, also in contact with the sediment.

In a recent study (Jansen *et al.* 1994) it was found that the benthic single roving electrode configuration produced much higher quality data than using a benthic gradient array. Examples of data acquired using the two different methods over the same profile are shown in Figure 8.22. In the benthic gradient array dataset (Figure 8.22A), one main negative anomaly can be seen at location 410 ft north. The same feature is evident on the benthic single roving electrode data (Figure 8.22B). However, an additional feature is clearly seen at location 640 ft north. Other features are evident on both datasets but appear to be less significant but do demonstrate the degree of repeatability, despite using a different electrode configuration. The reason the potential increases with the roving electrode is related to the changing distance from the remote electrode. In the gradient array, it is the potential measured across the pair of electrodes at a separation of 40 ft (12.2 m). The units of measurement should be given as mV/unit length (e.g. per dipole length). In the roving electrode case, it is not a complicated task to remove the effects of distance on the data to residualise the data in order to highlight anomalous zones.

Figure 8.22 (*opposite*) Examples of boat-borne SP profiling along a test line in a fresh-water filled reservoir, using (A) a benthic gradient array with a 40 ft (12.2 m) electrode spacing, and (B) a benthic single roving electrode with remote reference electrode. From Jansen *et al.* (1994), by permission